The combined impact of canopy stability and soil NOx exchange on ozone removal in a temperate deciduous forest

Auke Visser[1], Laurens Ganzeveld[2], Angelo Finco[3], Maarten C. Krol[4], Riccardo Marzuoli[3], and K. F. Boersma[1]

[1]Wageningen University
[2]Wageningen University and Research Centre
[3]Università Cattolica del Sacro Cuore
[4]Utrecht University

November 21, 2022

Abstract

Dry deposition is an important ozone sink that impacts ecosystem carbon and water cycling. Ozone dry deposition in forests is regulated by vertical transport, stomatal uptake, and non-stomatal processes including chemical removal. However, accurate descriptions of these processes in deposition parameterizations are hindered by sparse observational constraints on individual sink terms. Here we quantify the contribution of canopy-atmosphere turbulent exchange and chemical ozone removal by soil-emitted nitric oxide (NO) to ozone deposition in a North-Italian broadleaf deciduous forest. We apply a multi-layer canopy exchange model to interpret campaign observations of nitrogen oxides (NO_x=NO+NO2) and ozone exchange above and inside the forest canopy. Two state-of-science parameterizations of in-canopy vertical diffusivity, based on above-canopy wind speed or stability, do not reproduce the observed exchange suppressed by canopy-top radiative heating, resulting in overestimated dry deposition velocities of 10-19\% during daytime. Applying observation-derived vertical diffusivities in our simulations largely resolves this overestimation. Soil emissions are an important NOx source despite the observed high background NOx levels. Soil NOx emissions decrease the gradient between canopy and surface layer NOx mixing ratios, which suppresses simulated NOx deposition by 80% compared to a sensitivity simulation without soil emissions. However, a sensitivity analysis shows that the enhanced chemical ozone sink by reaction with soil-emitted NO is offset by increased vertical ozone transport from aloft and suppressed dry deposition. Our results highlight the need for targeted observations of non-stomatal ozone removal and turbulence-resolving deposition simulations to improve quantification and model representation of forest ozone deposition.

The combined impact of canopy stability and soil NO_x exchange on ozone removal in a temperate deciduous forest

Auke J. Visser[1], Laurens N. Ganzeveld[1], Angelo Finco[2], Maarten C. Krol[1,3], Riccardo Marzuoli[2], K. Folkert Boersma[1,4]

[1]Wageningen University, Meteorology and Air Quality Section, Wageningen, the Netherlands
[2]Università Cattolica del Sacro Cuore, Department of Mathematics and Physics, Brescia, Italy
[3]Utrecht University, Institute for Marine and Atmospheric Research Utrecht, Utrecht, the Netherlands
[4]Royal Netherlands Meteorological Institute, R&D Satellite Observations, De Bilt, the Netherlands

Key Points:

- We use a multi-layer canopy-atmosphere exchange model to interpret ozone flux observations inside and above a North-Italian forest
- Two state-of-science vertical exchange parameterizations do not capture in-canopy stable stratification suppressing ozone deposition
- Soil nitric oxide emissions do not increase ozone deposition due to compensating effects by deposition and transport

Corresponding author: A.J. Visser, `auke.visser@wur.nl`

Abstract

Dry deposition is an important ozone sink that impacts ecosystem carbon and water cycling. Ozone dry deposition in forests is regulated by vertical transport, stomatal uptake, and non-stomatal processes including chemical removal. However, accurate descriptions of these processes in deposition parameterizations are hindered by sparse observational constraints on individual sink terms. Here we quantify the contribution of canopy-atmosphere turbulent exchange and chemical ozone removal by soil-emitted nitric oxide (NO) to ozone deposition in a North-Italian broadleaf deciduous forest. We apply a multi-layer canopy exchange model to interpret campaign observations of nitrogen oxides (NO_x=NO+NO_2) and ozone exchange above and inside the forest canopy. Two state-of-science parameterizations of in-canopy vertical diffusivity, based on above-canopy wind speed or stability, do not reproduce the observed exchange suppressed by canopy-top radiative heating, resulting in overestimated dry deposition velocities of 10-19% during daytime. Applying observation-derived vertical diffusivities in our simulations largely resolves this overestimation. Soil emissions are an important NO_x source despite the observed high background NO_x levels. Soil NO_x emissions decrease the gradient between canopy and surface layer NO_x mixing ratios, which suppresses simulated NO_x deposition by 80% compared to a sensitivity simulation without soil emissions. However, a sensitivity analysis shows that the enhanced chemical ozone sink by reaction with soil-emitted NO is offset by increased vertical ozone transport from aloft and suppressed dry deposition. Our results highlight the need for targeted observations of non-stomatal ozone removal and turbulence-resolving deposition simulations to improve quantification and model representation of forest ozone deposition.

Plain Language Summary

Ozone is a harmful air pollutant that impacts human and ecosystem health. Ozone can be removed by forest ecosystems as a result of air transport into forests followed by plant ozone uptake or chemical removal, but quantifying these individual processes is difficult. We combine model simulations and treetop measurements to study the role of vertical forest-atmosphere air transport and chemical ozone removal inside the forest. We find that our model can only reproduce surface ozone removal if we account for suppressed transport as derived from observations. The soil is a substantial source of nitric oxide (NO) that reacts with ozone. According to our analysis, the presence of a soil NO source does not lead to increased ozone removal because other ozone sinks are reduced. Our results suggest that individual ozone removal processes in forests can best be studied using targeted observations and models that better resolve forest-atmosphere exchange.

1 Introduction

Removal of ozone at the land surface (ozone dry deposition) is an important component of the tropospheric ozone budget, accounting for 15-20% of the total tropospheric ozone sink (Hu et al., 2017; Young et al., 2018; Bates & Jacob, 2020). Ozone dry deposition occurs when air masses, transported downward by turbulent motions in the atmospheric boundary layer, come in contact with the land surface. Forests are particularly efficient ozone sinks (e.g., Hardacre et al., 2015): removal processes include plant uptake through stomata and various non-stomatal sinks such as external leaf surfaces and soils, and chemical removal in the canopy airspace (Fowler et al., 2009). Upon stomatal uptake, ozone may impact stomatal conductance and photosynthesis, reducing ecosystem carbon assimilation on large spatial scales (Ainsworth et al., 2012). Better quantitative estimates of stomatal and non-stomatal ozone sinks can improve understanding and quantification of the total land surface ozone sink and impacts on ecosystem carbon uptake driven by stomatal ozone uptake.

Stomatal uptake typically accounts for 40-90% of forest ozone uptake during the growing season (Fowler et al., 2009), but the contribution by individual sink terms is poorly constrained by parameterizations of land-atmosphere exchange in global and regional atmospheric chemistry models (Clifton et al., 2020). Multi-parameterization intercomparisons indicate that these uncertainties lead to a large spread in simulated ozone deposition (Wu et al., 2018; Visser et al., 2021). Likewise, Clifton et al. (2017) found that interannual variability in the ozone deposition velocity in a global atmospheric chemistry model was underestimated by a factor two compared to an 11-year ozone flux dataset, and attributed this to year-to-year variability in non-stomatal removal. Global model simulations of ozone deposition carry considerable uncertainty (Hardacre et al., 2015; Young et al., 2018), and an effort to quantify inter-model spread of ozone deposition in regional air quality models is currently underway (Galmarini et al., 2021). Altogether, these findings highlight the need for improved process understanding of ozone deposition. In this study, we focus on two of these uncertain processes: in-canopy turbulent exchange and ozone scavenging by soil-emitted nitric oxide (NO). These processes are not explicitly considered in commonly applied "big leaf" representations of dry deposition. Additionally, the scarcity of observational constraints on these processes limit our understanding of the contribution of these processes to forest ozone deposition.

Vertical mixing conditions inside forests can be different compared to those above the canopy, leading to an inversion at the canopy top or inside the canopy, regulated by meteorological conditions and forest structure (Russell et al., 2018). This can lead to a (partial) decoupling between the canopy and the overlying air layers, with implications for canopy-atmosphere gas exchange (e.g., Foken et al., 2012). For example, in-canopy inversions can lead to a missing soil carbon respiration contribution to above-canopy measurements of net ecosystem exchange of CO_2 (Jocher et al., 2018). For ozone, several studies suggest a dependence of ozone deposition on in-canopy turbulent mixing based on correlations between the deposition velocity and the friction velocity (e.g., Neirynck et al., 2012; Fares et al., 2014; El-Madany et al., 2017). Van Pul and Jacobs (1994) derived such a parameterization from measurements over maize crop, but its applicability to other land use categories remains uncertain. Multi-layer canopy-atmosphere exchange models typically simulate vertically resolved in-canopy and canopy-surface layer turbulent exchange based on K-theory (e.g., Ganzeveld, Lelieveld, Dentener, Krol, & Roelofs, 2002; Ashworth et al., 2015), which however has strong limitations when applied for rough surfaces such as forests (Bannister et al., 2022). Inferring in-canopy mixing conditions from observations requires vertical profile measurements of temperature and the sensible heat flux (e.g., Brown et al., 2020), which are not typically available at flux measurement sites. Therefore, the simplified representation of canopy-atmosphere exchange in current models and the sparse observational constraints limit our understanding of the role of turbulent mixing in canopy ozone removal.

Chemical ozone removal in plant canopies is another poorly constrained element of the ozone deposition sink. The canopy has a distinctly different photo-chemical regime compared to the surface layer affected by radiation extinction, emissions of soil NO and biogenic volatile organic compounds (BVOCs), as well as deposition processes. In big leaf parameterizations, it is common practice to emit soil NO directly into the surface layer after application of a canopy reduction factor, thereby only implicitly accounting for in-canopy NO_x removal. Therefore, these parameterizations do not account for the different photo-chemical regime inside the canopy. Observation-based studies indicate a widely varying contribution of chemical ozone removal by soil NO and BVOCs, that largely depends on site-specific characteristics such as soil and plant type, temperature, soil moisture and vapour pressure deficit (Fares et al., 2012; Rannik et al., 2012; Finco et al., 2018; Vermeuel et al., 2021). Due to decreasing anthropogenic emissions, agricultural and forest soils are becoming an increasingly important component of the European NO_x emission budget (Skiba et al., 2021), that contribute to ozone formation particularly during NO_x-limited ozone formation conditions (Visser et al., 2019). Soil-emitted

NO also act as an ozone sink inside forest canopies depending on the emission strength and canopy radiation extinction, leading to a locally NO_x-saturated ozone production regime. Commonly used parameterizations of soil-biogenic NO_x emissions in chemical transport models assume that forest soil NO emissions are relatively small compared to anthropogenic emissions, but are an important source of NO_x in pristine environments (Yienger & Levy, 1995). For example, Rummel et al. (2007) found that soil NO-ozone chemistry accelerates nighttime near-surface ozone loss in a tropical forest. In more polluted environments, nitrogen deposition accumulated over multiple years may substantially increase forest soil NO_x emissions (Pilegaard et al., 2006). Under such circumstances, soil NO-ozone chemistry may explain a considerable part of total ozone deposition even during daytime (Dorsey et al., 2004; Duyzer et al., 2004).

In this study, we aim to investigate the combined impact of canopy stability and soil NO emissions in the canopy airspace on ozone fluxes. We interpret field campaign observations of vertical gradients in ozone uptake in the North-Italian Bosco Fontana forest, experiencing substantial NO_x and ozone air pollution (Finco et al., 2018). This analysis of field observations is supported by observation-driven simulations with the Multi-Layer Canopy-CHemistry Exchange Model (Ganzeveld, Lelieveld, Dentener, Krol, & Roelofs, 2002; Visser et al., 2021). Specifically, we address the following research questions for a temperate mid-latitude forest:

1. How does the representation of vertical exchange in a multi-layer canopy model affect simulated canopy ozone uptake?
2. What is the contribution of soil and canopy-top NO_x fluxes to observed NO_x mixing ratios inside and above the canopy?
3. What is the contribution of NO_x-ozone chemistry to in-canopy ozone removal under different model representations of vertical exchange?

2 Data and Methods

2.1 Observations

We use atmosphere-biosphere exchange measurements obtained during an observational campaign in June-July 2012 at the Bosco Fontana deciduous forest in northern Italy (45.20°N,10.74°E) (Finco et al., 2018). This campaign took place within the European project ECLAIRE (Effects of Climate Change on Air Pollution Impacts and Response Strategies for European Ecosystems). This forested site is situated in the Po Valley, in a 235 ha natural reserve composed primarily of *Carpinus betulus L.* and *Quercus robur L.*, and the average canopy height is 26 m above ground level (Gerosa et al., 2017).

The Po Valley is characterized by warm summers and high concentrations of ozone and nitrogen oxides. Under such conditions, hydrological interactions leading to droughts might reduce the land surface ozone sink, which can exacerbate ozone air pollution (Lin et al., 2020). The summer of 2012 was characterized by slightly drier meteorological conditions ($\pm 1\sigma$) compared to the long-year average around Bosco Fontana, while the area south of the Po Valley experienced dry conditions (Fig. 1b, more details can be found in Supplementary Text S1). The stomatal ozone flux does not exceed 3 nmol m^{-2} s^{-1} and is up to 50% lower compared to the multi-year summer average value (Fig. 1). This is likely caused by stomatal closure as a result of drought conditions. In the (pre-)alpine regions north of Bosco Fontana, conditions are slightly wetter than average, and stomatal ozone fluxes are higher (>4 nmol m^{-2} s^{-1}) compared to the south, with no clear indication of a regional anomaly (Fig. 1b). We therefore deem these observations representative for typical summer conditions in North Italy.

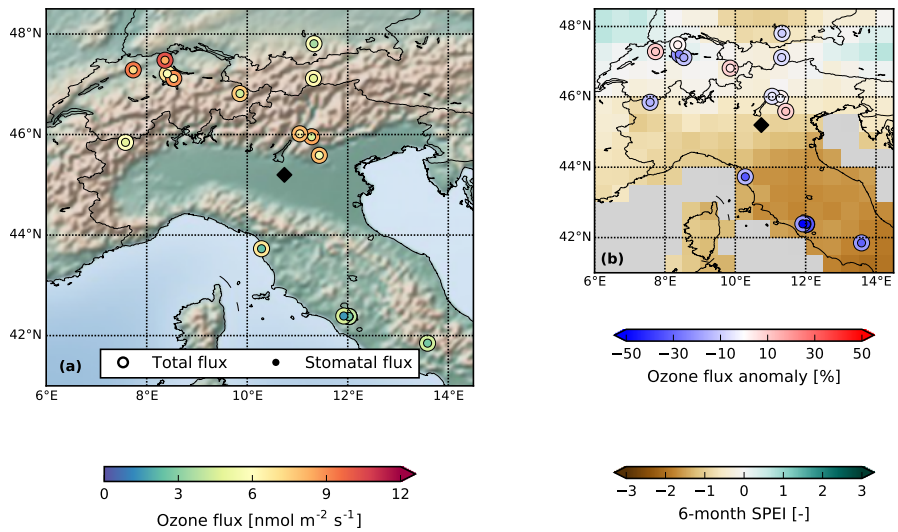

Figure 1. Summer 2012 ozone fluxes around northern Italy in a spatio-temporal context. Panel a: June-August average daytime total (outer circles) and stomatal (inner circles) ozone fluxes derived from observations at FLUXNET locations (data from Ducker et al., 2018). Panel b: July-August normalized 3-month SPEI anomaly (gridded data, derived from `https://spei.csic.es/index.html`, last access 24 March 2022), where negative (positive) values indicate drier (wetter) than average conditions, and the total and stomatal ozone flux relative anomaly compared to the observational record at the FLUXNET location. Bosco Fontana is indicated with a black diamond in both figures. See Supplementary Text S1 for details on the SPEI and SynFlux data analysis.

We here focus on the period of 24 June-11 July 2012, when temperature, wind speed, humidity, ozone and NO_x concentrations as well as fluxes of sensible heat and ozone were measured along a vertical profile inside and above the canopy at the Bosco Fontana site. Specifically, measurements were performed at two heights above the canopy top (41m and 32m), at the interface layer between the canopy and the surface layer (24m) and at two heights inside the canopy (8m and 16m). More details on the observational setup and flux data processing can be found in Finco et al. (2018).

2.2 The Multi-Layer Canopy-CHemistry Exchange Model (MLC-CHEM)

We perform biosphere-atmosphere trace gas exchange simulations using the Multi-Layer Canopy-CHemistry Exchange Model (MLC-CHEM). This model simulates atmosphere-biosphere exchange fluxes and vertical profiles of trace gases, and includes a representation of biogenic volatile organic compounds (BVOC) emissions (Guenther et al., 2012) and soil NO emissions (Yienger & Levy, 1995), in-canopy vertical mixing, a complex chemistry scheme (CBM-IV) and dry deposition of atmospheric compounds (Ganzeveld & Lelieveld, 1995; Ganzeveld et al., 1998). Stomatal conductance is calculated using the assimilation-stomatal conductance model A-g_s (Ronda et al., 2001), with parameter settings based on the observation-driven values derived by Visser et al. (2021). In this study, we force MLC-CHEM with canopy-top observations of net shortwave radiation, temperature, relative humidity, wind speed, friction velocity and surface-layer NO, NO_2 and ozone mixing ratios. MLC-CHEM simulates in-canopy mixing ratios and fluxes of these species as affected by the aforementioned sources and sinks inside the canopy. We further highlight

MLC-CHEM's representation of vertical exchange and soil NO emissions in the sections below.

In the set-up of MLC-CHEM in this study, the model consists of three layers: one bulk atmospheric surface layer, and a crown and understory layer that together represent the forest canopy. This set-up of the model has also been coupled to large-scale atmospheric chemistry models (Ganzeveld, Lelieveld, Dentener, Krol, Bouwman, & Roelofs, 2002; Ganzeveld et al., 2010). In-canopy radiation is expected to display large gradients between canopy-top and soil, and therefore processes affected by radiation (photolysis and biogenic emissions) are calculated in more vertical detail using four layers. Although MLC-CHEM can in principle be applied at a higher vertical resolution (i.e. with more than two canopy layers), we can only derive vertical transport from observations at two heights inside the canopy (see Section 2.3.3 and Figure 2). This motivates our use of the two-layer version in this study.

2.3 Vertical mixing in MLC-CHEM

We here test two methods of simulating turbulent exchange between atmosphere and the canopy, and compare these to exchange simulations with observation-derived vertical exchange. These representations will be introduced in this section, and are schematically visualised in Figure 2.

2.3.1 Reference parameterization of turbulent exchange (REF)

MLC-CHEM's default parameterization of turbulent exchange between canopy and the surface layer derives the surface-layer to upper canopy eddy diffusivity (denoted as $K_{H,sl}$) by integrating the aerodynamic conductance over the difference in reference height between the surface layer and the upper canopy layer, following Monin-Obukhov Similarity Theory. The in-canopy eddy diffusivity ($K_{H,cl}$), used to calculate turbulent exchange between the crown layer and the understory layer, is then derived by scaling $K_{H,sl}$ with the in-canopy wind speed profile (Ganzeveld, Lelieveld, Dentener, Krol, & Roelofs, 2002):

$$K_{H,cl} = K_{H,sl} \frac{0.5(u(l) + u(l-1))}{0.5(u(1) + u(0))}. \tag{1}$$

where $u(l)$ is the horizontal wind speed at layer l (index values 0,1,2 represent the bulk surface layer, the upper canopy layer and the lower canopy layer, respectively, as shown in Fig. 2). The simulated in-canopy wind speed decreases exponentially as a function of canopy height and canopy-specific attenuation coefficients (Cionco, 1978). Figure 2 displays typical mid-day values of the vertical diffusivity as derived from MLC-CHEM. During typical summer afternoon conditions characterized by efficient vertical mixing above the canopy, in-canopy K_H is typically a factor ± 7 lower than canopy-top K_H due to the scaling by the in-canopy wind speed.

2.3.2 Near-field theory (NFT)

We additionally apply a parameterization based on near-field theory (Raupach, 1989), which has resulted in improved surface ozone simulations with an online chemistry transport model (CTM) over forested regions in the United States (Makar et al., 2017). This formulation accounts for a decrease in the turbulent mixing intensity inside and above the forest with respect to the reference height of the lowermost model layer, resulting from obstruction of air flow due to the presence of trees. In this parameterization, $K_{H,sl}$ in the lowermost model layer of the CTM is scaled down towards the land surface as a function of canopy height, friction velocity and the Obukhov length. Figure 2 shows how the NFT vertical diffusivity decreases towards the surface in this formulation as a result

of canopy influences on turbulence intensity. K_H at the canopy-top is particularly smaller in NFT compared to the reference parameterization in MLC-CHEM (REF). In-canopy K_H is relatively similar in both formulations.

2.3.3 Observation-inferred turbulent exchange derivation (INF)

Thirdly, we derive the the turbulent exchange coefficient from observations following K-theory. This theory relates the observed sensible heat flux to the obseved vertical potential temperature gradient via the vertical diffusivity coefficient K_H:

$$H(z) = -K_H(z)\frac{\delta\theta(z)}{\delta z} \tag{2}$$

where $H(z)$ is the observed sensible heat flux at height z and $\frac{\delta\theta(z)}{\delta z}$ is the vertical potential temperature gradient at height z, inferred from temperature measurements above and below z. This slope is derived by fitting potential temperature to the curve $\theta = a + b \times ln(z) + c \times ln(z)^2$ (Mölder et al., 1999; Brown et al., 2020). We here apply the vertical diffusivity derived from observed vertical profiles of temperature and the sensible heat flux in our simulations of ozone and NO_x canopy-atmosphere exchange, assuming that exchange coefficients of these gases resemble the exchange coefficient of heat. We will revisit this assumption in the discussion, by a comparison with exchange coefficients derived from vertical gradients of ozone concentrations and fluxes.

We calculate $K_H(z)$ at two different heights within the canopy. K_H is calculated at the canopy-surface layer interface from 30-minute averages of sensible heat fluxes measured at 24m and temperature gradients between 16m and 32m. In-canopy K_H is derived from 30-minute averages of sensible heat fluxes measured at 16m and temperature gradients between 8m and 24m. Figure 2 displays the typical mid-day K_H range as derived from observations. Note that we apply $K_{H,24m}$ for simulating exchange at the canopy-top, so these values are shown at z=26m. $K_{H,16m}$ is used for simulating vertical exchange between the crown and understory layers (z=13m). The observation-inferred K_H is lower than REF and NFT at the canopy-top, and the mid-canopy values of REF and NFT approximately coincide with the upper value of the observation-inferred K_H range.

2.4 Soil NO_x exchange

We perform an initial evaluation of MLC-CHEM-simulated NO_x mixing ratios in the understory to understand the role of soil NO_x exchange on observed NO_x mixing ratios at Bosco Fontana. A simulation with the default deciduous forest soil NO emission factor from (Yienger & Levy, 1995) results in an emission strength of 0.2-0.6 ng N m^{-2} s^{-1} (Supp. Fig. S2a). This is substantially lower than the site-derived emission flux of 20.8 ng N m^{-2} s^{-1}, based on enclosure chamber measurements directly above the Bosco Fontana forest floor (Finco et al., 2018). As a result, MLC-CHEM-simulated understory NO_x mixing ratios using the default deciduous forest emission factor are underestimated by 2.1 ppb (27%) on average (Supplementary Fig. S2c).

However, imposing the observation-derived soil NO emission flux in MLC-CHEM leads to an overestimation of understory NO_x mixing ratios by 3.1 ppb (37%) compared to observations, reflecting NO_x accumulation (Supplementary Fig. S2c). These over-estimations in simulated lower-canopy [NO_x] result partly from an underestimated NO_2 deposition sink in MLC-CHEM (1-6 ng N m^{-2} s^{-1}) that is more than a factor two smaller compared to the observation-derived soil NO_2 deposition flux of ±14 ng N m^{-2} s^{-1} (Finco et al., 2018). A sensitivity test assuming a strongly enhanced soil uptake efficiency of NO_2, by reducing MLC-CHEM's NO_2 soil uptake resistance from 600 to 100 s m^{-1}, does not strongly increase simulated soil NO_2 deposition. Additionally, there are strong observed vertical gradients in NO_x mixing ratios near the soil, reflecting strongly stable conditions

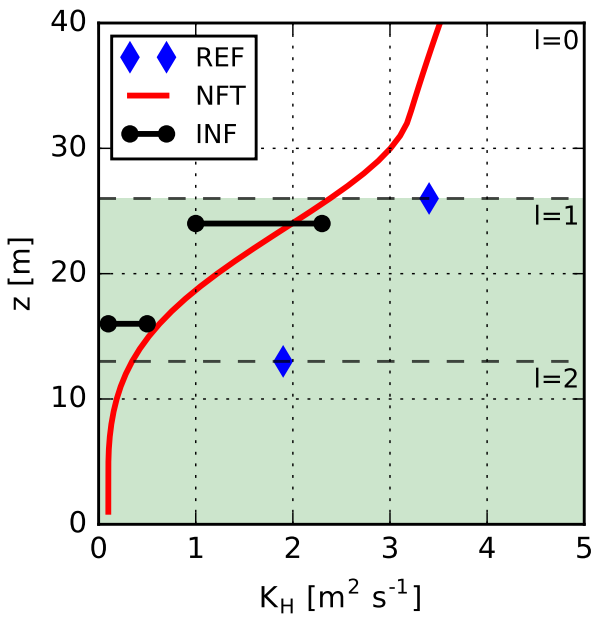

Figure 2. Schematic representation of typical afternoon vertical profiles of vertical diffusivity (K_H) in the Bosco Fontana forest (indicated by the green shaded area) in an unstable mixing regime. The reference MLC-CHEM vertical mixing parameterization (REF) is shown in blue diamonds and the near-field theory parameterization (NFT) is indicated by the red line. These profiles are calculated using $u_* = 0.5$ m s^{-1}, u = 2 m s^{-1}, $K_H(z_{ref}) = 4$ m^2 s^{-1} (at a reference height of 50 m), $r_a = 20$ s m^{-1}. Solid black lines and points show the mid-day (12-15 h LT) range of observation-inferred K_H values at two different heights. Dashed black lines indicate the interface between model layers in MLC-CHEM. The index l (varying from 0-2) refers to the model layers in Equation 1.

Table 1. Configuration of MLC-CHEM simulations.

Experiment	K_H method	$E_{NO,soil}$ [ng N m^{-2} s^{-1}]	$r_{soil}(NO_2)$ [s m^{-1}
1	REF	0.2-0.6[a]	600
2	REF	8	600
3	NFT	8	600
4	INF	8	600
5	REF	0	10^5
6	NFT	0	10^5
7	INF	0	10^5

[a] Diurnal range, peaking in the afternoon

and NO_x loss due to chemical removal and soil deposition, which are not represented in MLC-CHEM's understory layer with a thickness of 13 m. This indicates that a substantial part of the soil-emitted NO_x does not escape the air layer directly above the soil.

In order to infer the contribution of soil NO_x exchange to observed NO_x mixing ratios at the reference height of MLC-CHEM's understory layer (z=6.5 m), we study the sensitivity of simulated understory NO_x to the soil NO emission flux. By comparison with observed NO_x mixing ratios in the understory, we find that application of a reduced soil NO emission strength of 8 ng N m^{-2} s^{-1} minimizes the mismatch between simulated and observed understory NO_x (Supplementary Fig. S2c), and we therefore choose this value to represent the effect of soil NO_x exchange on canopy ozone uptake for our simulations.

2.5 Setup of the numerical experiments

In order to answer our research questions, we modify the representation of in- and above-canopy vertical mixing, as well as soil NO_x exchange, in MLC-CHEM. The reference simulation (experiment 1) applies the model's reference vertical diffusivity formulation (REF), a default temperate forest soil NO emission factor (Yienger & Levy, 1995) and the standard soil NO_2 uptake resistance (Ganzeveld & Lelieveld, 1995). In experiments 2-4, we modify MLC-CHEM's vertical exchange formulation as explained in Section 2.3. We use the effective soil NO emission flux that best represents soil effects on lower-canopy NO_x mixing ratios and the default NO_2 uptake resistance (Section 2.4). In experiments 5-7, we deactivate soil NO emissions and soil NO_2 deposition to quantify the effect of soil NO_x exchange on in-canopy NO_x mixing ratios and ozone deposition.

3 Results

3.1 Vertical exchange

We start our analysis by examining temporal variability in the observation-derived vertical diffusivity (K_H) and its relation to in- and above-canopy stability. Figure 3 displays the stability regimes in the surface layer and the canopy. Stably stratified conditions occur frequently inside the canopy even during daytime (Fig. 3), resulting from radiative heating of the canopy-top and a closed canopy structure that prevent the warm above-canopy air from entering the canopy airspace (Finco et al., 2018). Observation-inferred K_H at the interface between the canopy and the overlying air layer (z=24 m) peaks at 2.4 m^2 s^{-1} at 15:30 LT (Fig. 4b), coinciding with prevailing unstable mixing conditions above the canopy (Fig. 3). The campaign-average diurnal cycle of the observation-derived K_H inside the canopy (z=13 m) is characterized by lower values throughout the day (up to 0.5 m^2 s^{-1}, Fig. 4d), reflecting the decrease in vertical mixing inside the for-

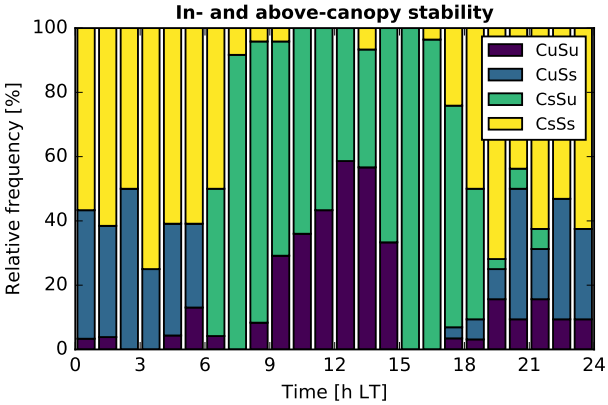

Figure 3. Occurrence of in- and above-canopy stability classes during the observational time period (24 June-12 July, 2012). Data were separated into four stability classes, based on stability parameter $\frac{z}{L}$ as unstable (lowercase u, $\frac{z}{L} < 0$) or stable (lowercase s, $\frac{z}{L} > 0$), as well as height of the observations, being representative of the surface layer (uppercase S, derived from observations at 32m) or inside the canopy (uppercase C, derived from observations at 16m).

est canopy (Fig. 2). Mid-canopy K_H derived from observations peaks at 11:30-12:00 LT (Fig. 4d), coinciding with predominantly unstable conditions inside and above the canopy.

Contrary to the observations, simulated K_H according to the REF approach in MLC-CHEM follows a symmetric diurnal profile peaking at 13:00 LT (Fig. 4b), which is substantially larger compared to the observation-inferred K_H during daytime. The K_H overestimation results from the simplified K_H derivation in this model setup (see Section 2.3.1). As a result, REF-simulated vertical exchange at the canopy-top is overestimated compared to observation-inferred K_H (Fig. 4b). The REF-simulated in-canopy K_H shows substantial day-to-day variation due to its dependence on above-canopy wind speed (Section 2.3.1), and strongly overestimates K_H inside the canopy leading to well-mixed conditions inside the canopy during daytime in this simulation. As a result, vertical exchange is strongly overestimated in the REF vertical exchange representation in MLC-CHEM compared to observation-inferred vertical mixing during the observational campaign.

Canopy-top K_H from a simulation based on near-field theory (NFT) follows a similar diurnal cycle compared to REF, since NFT is derived from scaling down the REF-simulated vertical diffusivity to include effects of the roughness sublayer (see Section 2.3.2). The NFT-simulated K_H above the canopy is up to 3 m^2 s^{-1} lower compared to the REF simulation during mid-day, and in closer agreement with observation-inferred K_H values. Inside the canopy, the NFT-simulated K_H is also substantially lower compared to the REF K_H, and in closer agreement with observation-inferred values. However, NFT does also not reproduce the observed low afternoon K_H values indicative of stably stratified conditions inside the canopy. In the next section, we will evaluate the effects of these different representations of vertical diffusivity on the simulated ozone and NO_x profiles.

3.2 Effects of turbulent mixing on canopy ozone uptake

We analyze the effect of vertical mixing on ozone deposition via the simulated deposition velocity. In MLC-CHEM, vertical mixing affects the canopy-atmosphere transport of ozone and thus the ozone flux. V_dO_3 is diagnostically calculated from the ozone flux at the canopy-atmosphere interface and canopy-top ozone mixing ratios simulated by MLC-CHEM. Figure 5 displays the campaign-median ozone dry deposition velocity

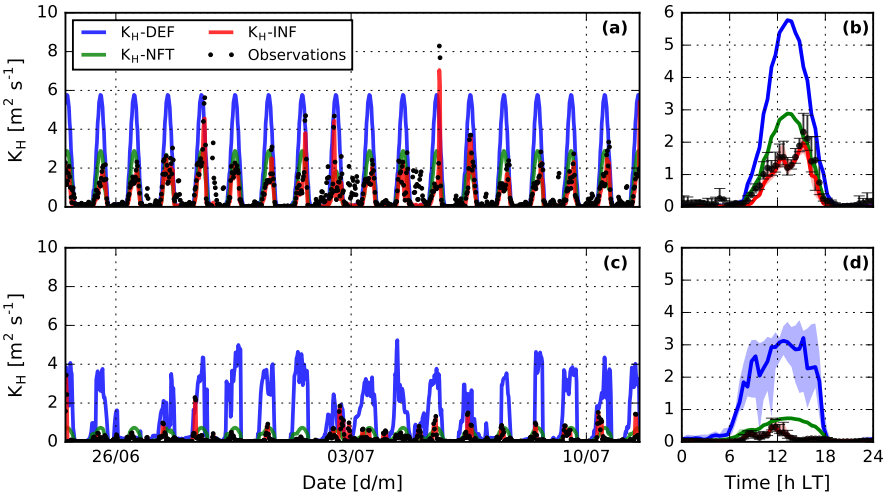

Figure 4. Time series (panels a,c) and campaign-average diurnal cycle (panels b,d) of vertical diffusivity at the canopy-surface layer interface (panels a,b) and 13 m, halfway the canopy (panels c,d), as derived from observations (black dots), and as calculated from three MLC-CHEM simulations (solid lines, see Section 2.3) Black lines and shaded areas indicate the inter-quartile range.

($V_d(O_3)$) diurnal cycle from observations and three MLC-CHEM simulations with different representations of vertical exchange. Observed $V_d(O_3)$ is characterized by nighttime values of 0.0-0.2 cm s^{-1}, followed by a sudden increase in the morning ($\pm$8 h LT) to its peak value, and a subsequent decrease throughout the day. Notably, the REF and NFT simulations strongly overestimate $V_d(O_3)$ at 5-8 h LT, while a simulation with the observation-derived representation of vertical exchange (INF) agrees better with observations during this time period. This coincides with overestimated K_H values in REF and NFT, particularly at mid-canopy, during the early morning (Fig. 4d). Neither simulation reproduces the daytime peak value occurring at 8 h LT, which reflects a sudden change from stable to unstable stratification in the upper canopy. The spread in observed $V_d(O_3)$ at this time is high, indicating that the timing of the change to unstable conditions varies from day to day, or a possible role of intermittent exchange. The REF and NFT simulations overestimate daytime $V_d(O_3)$ (9-16 h LT) by 19% and 10%, respectively. INF reproduces daytime $V_d(O_3)$ within 5% of the observations due to accounting for a (partial) decoupling between the canopy and the surface layer.

Despite distinct differences in the simulated diurnal cycle, effects of vertical exchange on MLC-CHEM's performance (shown in Table 2) are small. The similar model performance metrics reflect the compensating effects of model overestimations and underestimations during different stages in the diurnal cycle, as discussed above. The effect of constraining the simulations with observation-derived vertical exchange most strongly reduces overestimations in the simulated ozone flux, as INF reduces the model overestimations from 13-16% to 8% (Table 2). When analyzing skill scores for 9-15 h LT, when unstable conditions inside and above the canopy are more prevalent, the MBE is markedly lower in the INF simulation (0.7 nmol m^{-2} s^{-1}) compared to the REF and NFT simulations (4.3 and 3.2 nmol m^{-2} s^{-1}, respectively). Hence, vertical exchange only minimally affects canopy ozone uptake averaged over the entire day, but the effects are substantial during time periods characterized by (partial) decoupling between canopy and the overlying atmospheric layers.

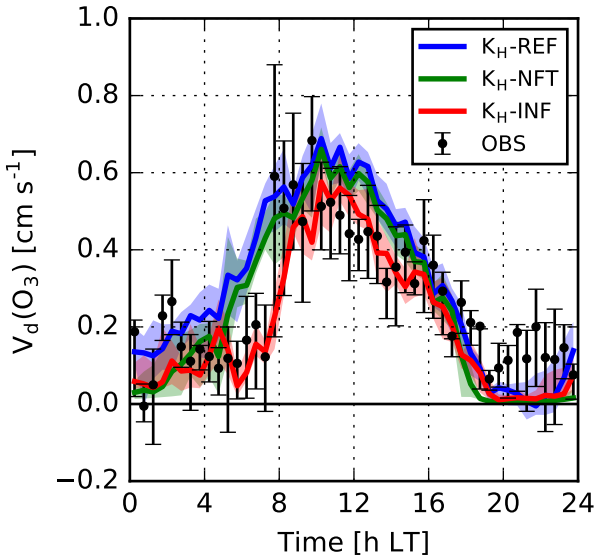

Figure 5. Campaign-median diurnal cycle of the ozone dry deposition velocity derived from observations (black points and whiskers), and simulated by MLC-CHEM with three different K_H derivations: MLC-CHEM's reference vertical diffusivity description (REF), near-field theory (NFT) and observation-inferred K_H (INF). The observation-inferred deposition velocity ($V_d(O_3) = \frac{F_{O_3}}{[O_3]}$) at the canopy-atmosphere interface (26 m) is derived by linear interpolation between observations at 24m and 32m.

Table 2. Model performance statistics of the simulated ozone flux in three MLC-CHEM simulations with different representations of vertical exchange. The table includes several common statistical model performance indicators (MBE, RMSE, r^2, slope and intercept of the linear regression fit through simulations and observations (s,i), as well as the index of agreement d (Willmott, 1982) and the fraction of simulated data points overestimated and underestimated by a factor larger than 2 (f>2× and f<2×), respectively). The unit is nmol m^{-2} s^{-1}, unless indicated otherwise.

	MBE	RMSE	r^2 [-]	s [-], i	d [-]	f>2× [-]	f<2× [-]
REF	1.61	5.5	0.45	0.69, 3.73	0.80	0.16	0.16
NFT	0.75	5.1	0.47	0.70, 2.86	0.82	0.13	0.22
INF	-0.18	4.9	0.45	0.60, 2.63	0.81	0.08	0.23

3.3 Effects of soil NO_x exchange on the canopy NO_x budget

Biosphere-atmosphere exchange of NO_x can be bi-directional (i.e. emission or deposition), depending on the difference between above- and below-canopy NO_x mixing ratios. Generally, the canopy-atmosphere NO_x flux is downward in (forested) regions with high background NO_x mixing ratios, regardless of the soil NO source strength (Ganzeveld, Lelieveld, Dentener, Krol, Bouwman, & Roelofs, 2002). Elevated NO_x mixing ratios observed at Bosco Fontana (up to 16 ppb in the morning and 4 ppb in the afternoon) therefore suggest that NO_x deposition to the forest canopy is expected to prevail at this site. The observed exchange of NO_x at the soil interface is bi-directional (NO emissions, NO_2 deposition), resulting in a substantial net upward NO_x flux (Finco et al., 2018, see also Sect. 2.4). We infer the contribution of soil NO_x exchange to in-canopy NO_x mixing ratios by comparing an MLC-CHEM simulation with observation-inferred vertical exchange (INF) to an experiment with deactivated soil NO_x exchange (experiments 4 and 7 in Table 1). Figure 6 displays observed and MLC-CHEM-simulated upper- and lower-canopy NO_x mixing ratios. As expected, the effect of soil NO_x exchange is largest in the understory, with simulated enhancements in NO_x mixing ratios of 0.6 ppb during daytime to 7.5 ppb at night due to soil NO_x exchange (Fig. 6b). Additionally, the simulation without soil NO_x exchange does not lead to nighttime NO_x accumulation in the canopy, and an underestimation of [NO_x] by >5 ppb during nighttime. Our sensitivity simulation suggests that the soil contributes on average 45% to observed mixing ratios in the understory. The net upward soil NO_x flux additionally affects the simulated diurnal course of lower-canopy NO_x mixing ratios, as the observed evening increase rate in NO_x mixing ratios is absent in the simulation without soil NO_x exchange.

Soil NO_x has a smaller effect on NO_x mixing ratios in the upper canopy layer compared to the understory. NO_x mixing ratios are lower by 0.1 ppb (daytime) up to 3.2 ppb (nighttime) in the simulation without soil NO_x exchange (Fig. 6a), and we infer that the soil contributes on average 21% to NO_x mixing ratios in this layer. The soil contribution is lowest during mid-day, when vertical exchange between the upper canopy and the overlying air layer is intense while mixing between the two canopy layers is suppressed (Fig. 4b,d). Note here that the NO_x concentrations in MLC-CHEM's surface layer are nudged to observations at 32 m. The similarity in the shape of the simulated diurnal cycles suggests that diurnal variation in upper-canopy NO_x mixing ratios is largely driven by the canopy-top NO_x flux. The two simulations diverge after 16 h LT, when the upper canopy becomes stably stratified, which indicates a substantial contribution of the soil to upper-canopy NO_x levels even at this site with a large NO_x source from advection.

Canopy-atmosphere NO_x exchange is strongly affected by soil NO_x exchange. Figure 7 displays campaign-median diurnal cycles of simulated canopy-top NO_x fluxes with and without considering the contribution by soil NO emissions. The simulated daytime upward canopy-top NO flux is higher by up to 3 ng N m^{-2} s^{-1} due to soil NO_x exchange (Fig. 7a). In both simulations, the canopy remains a net sink of NO_2 due to the high background levels observed at this site. However, canopy uptake of NO_2 is reduced due to the effect of soil NO_x emissions (Fig. 7b), and even changes in sign at night, as mixing of soil-emitted NO_x into the canopy layers reduces the gradient between canopy and the overlying air layer. As a result of the changing vertical gradient in NO_x mixing ratios between the canopy layers and the surface layer, considering soil NO_x exchange in MLC-CHEM reduces the canopy-top NO_x fluxes by on average 4.5 ng N m^{-2} s^{-1} (-79.8%). This analysis highlights the importance of accounting for soil NO_x exchange for accurately simulating NO_x deposition in larger-scale models for relatively polluted regions.

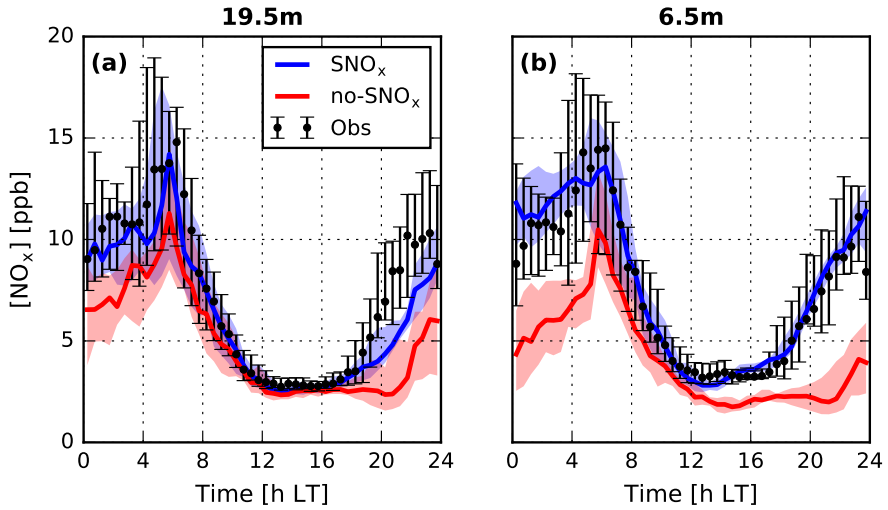

Figure 6. Campaign-median diurnal cycle of NO_x mixing ratios the reference heights of the two canopy layers, as simulated by MLC-CHEM (with observation-inferred vertical mixing) with (SNO_x, blue line) and without (no-SNO_x, red line) soil NO_x exchange. Observations at 19.5m are derived by vertical interpolation of measurements at 8 and 24m, while observations at 5m are directly compared to model output at 6.5m. Points and solid lines display the mean, and whiskers and shaded area display the inter-quartile range.

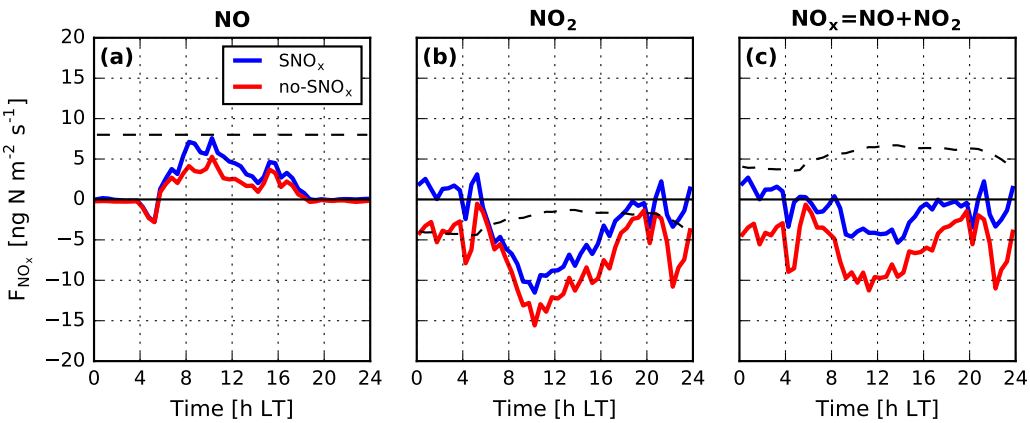

Figure 7. Canopy-top (26 m) fluxes of NO, NO_2 and NO_x simulated by MLC-CHEM with (SNO_x) and without (no-SNO_x) soil NO_x exchange, and using the observation-derived vertical diffusivity in both simulations (experiments 4 and 7 in Table 1). The black dashed lines indicate the soil fluxes for the SNO_x simulation.

3.4 Canopy reduction of NO_x

The simulated canopy-top NO flux is generally smaller than the soil NO flux at Bosco Fontana (Fig. 7), which reflects in-canopy NO_x loss. Many large-scale models do not explicitly represent canopy processes, and account for this decrease in the effective contribution by soil NO emissions to atmospheric NO_x mixing ratios by applying a canopy reduction factor (CRF) to account for in-canopy removal of the emitted NO_x by NO_2 deposition (Yienger & Levy, 1995). When above-canopy NO_x mixing ratios are smaller compared to the in-canopy NO_x mixing ratio, this CRF has a value between 0-1 (Yienger & Levy, 1995), e.g. ± 0.75 for midlatitude deciduous forest (Vinken et al., 2014). However, for high-NO_x regions such as northern Italy, an alternative definition of the CRF is more appropriate.

This alternative CRF is derived as the ratio between above-canopy and above-soil NO_x fluxes (Ganzeveld, Lelieveld, Dentener, Krol, Bouwman, & Roelofs, 2002), and reflects the role of in-canopy NO_2 deposition, chemical cycling, and the bi-directionality of canopy-atmosphere NO_x exchange. We derive a CRF of -0.24 (diurnal average), which indicates that the soil NO_x exchange flux is approximately 4 times higher than the simulated downward canopy-top NO_x flux. This negative estimate reflects that Bosco Fontana is a sink of NO_x, although much closer to zero compared to the CRFs of -10 - -1 found by Ganzeveld, Lelieveld, Dentener, Krol, Bouwman, and Roelofs (2002) over high-NO_x regions in the northern midlatitudes. This relatively small CRF inferred from our canopy-exchange simulations can largely be explained by the large soil NO emission flux at Bosco Fontana: Ganzeveld, Lelieveld, Dentener, Krol, Bouwman, and Roelofs (2002) used emission factors from Yienger and Levy (1995), which strongly underestimate soil NO emissions at Bosco Fontana (see Sect. 2.4). This study suggests caution for using large-scale soil NO emission algorithms (including canopy reduction factors) for interpreting the soil NO contribution to biosphere-atmosphere NO_x exchange in polluted environments.

3.5 Combined impact of vertical mixing and soil NO_x exchange on canopy ozone uptake

Figure 8 displays the campaign-median diurnal cycle of the total ozone flux as simulated by MLC-CHEM, using the three different representations of vertical exchange, with and without considering soil NO_x exchange. There is a decrease in the diurnal average ozone flux of 5-10% associated with the role of soil NO_x at this site, depending on the representation of vertical exchange. During daytime (5-20 h LT), the soil NO_x-induced decrease in ozone fluxes is smaller (3-4%), while the relative effect is largest during the night (>20%) due to low nighttime ozone fluxes. The in-canopy chemical ozone sink competes with other canopy ozone sinks, including stomatal uptake. However, the daytime stomatal ozone flux is reduced by only 1-3% due to the soil NO-ozone sink (not shown), suggesting that the substantial source of soil NO_x at Bosco Fontana is of minor importance for stomatal ozone uptake and flux-based metrics for ozone impacts on vegetation.

To further understand the weak sensitivity of the atmosphere-biosphere ozone flux to soil NO_x exchange, we analye differences in simulated ozone formation and removal tendencies with and without soil NO_x exchange. The tendencies (unit: ppb h^{-1}) are calculated as the contribution of vertical exchange, deposition and chemical transformation to changes in ozone mixing ratios at each time step, following Ganzeveld, Lelieveld, Dentener, Krol, and Roelofs (2002). Campaign-average diurnal cycles of these tendencies are shown in Supplementary Figure S3. The net upward soil NO_x exchange flux leads to changes in the diurnal variability in ozone tendencies, particularly in the lower canopy, but their diurnal variability remains similar. Therefore, we display diurnal averages of tendency changes due to soil NO_x exchange in Figure 9 for the three tested representations of vertical exchange, to explain the weak sensitivity of canopy-top ozone fluxes to soil NO_x exchange. Note that sinks result in negative ozone tendencies. As a result, an increased

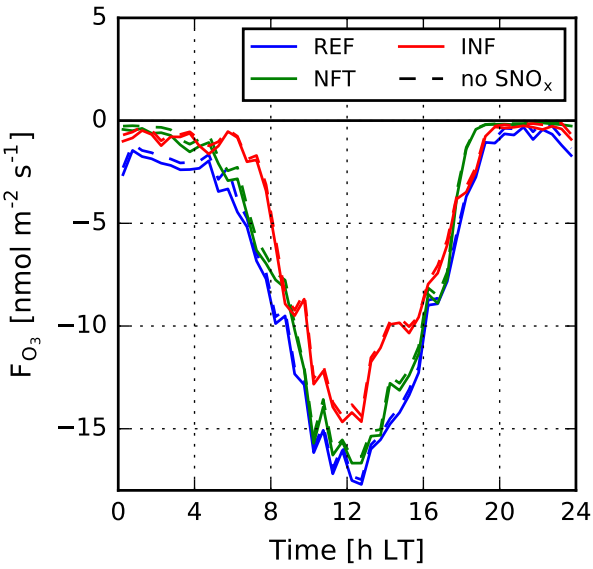

Figure 8. Campaign-median diurnal cycle of the total canopy ozone flux as simulated by MLC-CHEM using reference vertical exchange (REF), vertical exchange derived using near-field theory (NFT) and observation-inferred vertical exchange (INF). Solid lines indicate simulations with soil NO_x exchange, and dashed lines show simulations with deactivated soil NO_x exchange (i.e. soil NO emissions and soil NO_2 deposition).

sink leads to a negative tendency change, while a decreased sink leads to a positive tendency change.

The chemical ozone sink is increased due to reaction with soil-emitted NO, reflected by a negative tendency change for ozone in the lower canopy (Fig. 9). This introduces two compensating effects that both result in positive tendency changes: reduced deposition and increased vertical transport. Lower-canopy ozone deposition is reduced, because chemical removal and deposition are two competing sinks, acting on the ozone reservoir in the lower canopy. However, the reduced deposition sink does not fully compensate for the enhanced chemical ozone destruction. An additional compensating effect results from the dependence of vertical transport on the ozone gradient between the upper and lower canopy. The soil NO_x-induced chemical sink results in a larger vertical ozone gradient between the upper and lower canopy, and this increases vertical ozone transport into the lower canopy. These results do not strongly depend on the representation of vertical exchange (Figure 9). According to our analysis, reduced dry deposition and increased vertical transport together offset the enhanced lower-canopy ozone sink by reaction with soil NO.

4 Discussion

Our results show how vertical mixing conditions inside a forest differ from those in the atmospheric surface layer as a result of the presence of thermal inversions within the canopy. Accounting for these stability effects in the multi-layer canopy exchange model MLC-CHEM, by inferring the vertical diffusivity from observations (INF), leads to morning ozone deposition velocity decreases by up to 0.2-0.4 cm s^{-1} compared to two tested vertical exchange parameterizations in MLC-CHEM (REF and NFT), and in closer agreement with observations. In the afternoon, REF and NFT overestimate ozone deposition

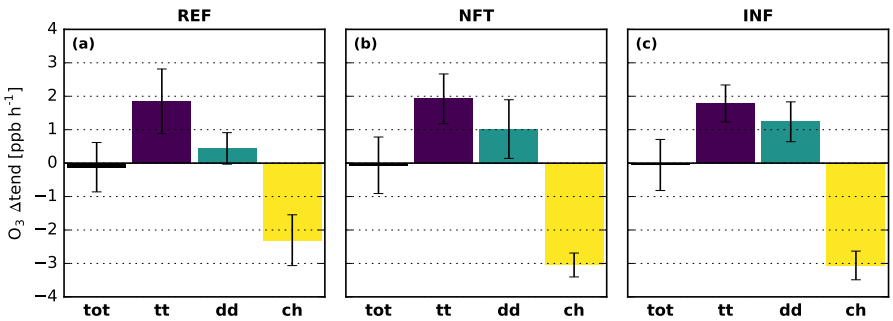

Figure 9. Change in lower-canopy ozone mean diurnal process tendencies as a result of soil NO_x exchange for three MLC-CHEM simulation pairs using REF-, NFT-, and INF-based vertical exchange (panels a,b,c, respectively). Displayed tendency differences (tendency with soil NO_x exchange minus tendency without soil NO_x exchange) are due to changes turbulent transport (tt), dry deposition (dd) and chemistry (ch), as well as the resulting total tendency change (tot). Error bars indicate the standard deviation of the mean diurnal process tendencies. Changes in simulated process tendencies due to soil NO_x exchange for the upper canopy are shown in Supplementary Figure S4.

flux by on average 4.3 and 3.2 nmol m^{-2} s^{-1}, respectively, while INF agrees better with observations (MBE = 0.7 nmol m^{-2} s^{-1}). Given the dependence of in-canopy turbulence on stand density and vertical leaf area distribution (e.g., Russell et al., 2018; Banerjee & Linn, 2018), this effect may be generalizable to closed forest canopies receiving high solar radiation. For these conditions, 3D atmospheric chemistry models, with highly parameterized vertical mixing inside and above forest canopies, could potentially overestimate atmosphere-biosphere exchange of ozone and other trace gases.

In our observation-based characterization of canopy-atmosphere exchange, we derived the vertical diffusivity from 30-minute averages of temperature and the sensible heat flux. This is a common method to infer canopy-atmosphere exchange from observations (e.g., Brown et al., 2020) that incorporates effects of thermal stability on vertical exchange inside the canopy and between the canopy and the surface layer. This is an advancement compared to conventional methods to simulate in-canopy transport, used in deposition parameterizations applied in large-scale chemistry-transport models (e.g., Van Pul & Jacobs, 1994), which are based on above-canopy turbulence intensity (via the friction velocity) and canopy density (via LAI). However, the K-theory approach based on average fluxes and gradients does not account for non-local, intermittent sources of turbulence (Raupach, 1989; Finnigan, 2000). Previous work found variable effects of coherent structures to observed canopy-top fluxes: Thomas and Foken (2007) found a resulting 4% error in eddy-covariance fluxes, while Steiner et al. (2011) reported a 44-65% contribution by coherent structures to the observed sensible heat flux.

The availability of ozone flux and mixing ratio observations along a vertical profile enables us to explore the similarity between K_H and a vertical diffusivity derived from 30-minute averages of ozone flux and mixing ratio observations (K_{O_3}), shown in Supplementary Figure S4. In the morning, K_{O_3} exceeds MLC-CHEM-simulated and observation-inferred K_H in the upper canopy (Supplementary Fig. S4a). Finco et al. (2018) find an enhanced ozone flux at the canopy-atmosphere interface, possibly resulting from a local enhancement in NO mixing ratios at the canopy-top transported to this height from the soil and the surface layer. During the morning, with a relatively large vertical transport timescale ($\tau_t \approx 10$ h, Fig. 10) compared to the smaller timescale of chemical ozone

loss by reaction with NO ($\tau_c \approx 1$ h, Fig. 10), we suspect that this enhanced flux will not change the ozone gradient between the canopy and the atmosphere, leading to an elevated K_{O_3} compared to K_H. During the afternoon, observation-derived values of K_H and K_{O_3} agree well, suggesting that chemical alteration of the ozone flux in the upper canopy dominantly occurs in the morning. Lower-canopy K_{O_3} exceeds K_H throughout the day (Supplementary Fig. S4b), reflecting enhanced ozone removal due to the reaction between soil-emitted NO and ozone.

Our results highlight that canopy exchange of NO_x is driven by the vertical gradient in NO_x mixing ratios between the canopy and the surface layer. Soil NO emissions are high at our North-Italian study site, possibly due to high nitrogen deposition (de Vries et al., 2021) leading to nitrogen accumulation in the soil. We estimate that these soil emissions offset the total NO_x deposition by 80%, and that soil-emitted NO is largely removed inside the forest. We conclude that information on canopy sources and sinks of NO_x, including soil NO emissions, is essential to understand the NO_x budget of forests, particularly in regions with high background levels of air pollution.

The campaign observations applied in this study indicate the presence of strong vertical gradients in NO_x and ozone mixing ratios in the lower canopy. Daytime NO_x mixing ratios measured directly above the soil are higher by up to 7 ppb compared to measurements at 5 m, while ozone mixing ratios above the soil (0.15 m) are ±20-55 ppb lower (Finco et al., 2018). These differences are caused by soil exchange processes (emissions of NO, deposition of NO_2 and ozone) and chemical reactions, amplified by the very stable stratification at this height. This near-surface effect is important for evaluating the contribution of soil emissions to the canopy NO_x exchange budget, as our results show that the soil NO_x flux inferred from above-soil enclosure chamber measurements cannot be reconciled with the observed NO_x mixing ratios at 6.5 m (Supplementary Fig. S2), likely indicating NO_x loss near the forest floor. Resolving these gradients requires an increased vertical resolution in MLC-CHEM. Our choice for a model with two canopy layers is justified by the applicability of this model version in regional/global models (Ganzeveld, Lelieveld, Dentener, Krol, & Roelofs, 2002; Ganzeveld et al., 2010), and the availability of observational constraints at two heights in the canopy.

To further investigate potential sub-grid vertical gradients, we derive mid-canopy lifetimes against vertical transport, chemical loss and deposition (Figure 10). If the lifetime against vertical transport (τ_t) is of a similar magnitude as the lifetime of other processes, replenishment is not sufficiently fast to counter chemical loss or deposition, leading to sharp vertical ozone gradients that are challenging to resolve in multi-layer canopy models. During the early morning and evening, τ_t is indeed of a similar or higher magnitude compared to τ_c and τ_d. During daytime, however, vertical ozone transport is much faster than chemical loss and deposition, indicating that the mid-canopy is well-mixed. However, sharp ozone and NO_x gradients occur directly above the soil (Finco et al., 2018), which occurs at the subgrid-scale in MLC-CHEM.

The aforementioned shortcomings could be addressed by application of a Large-Eddy Simulation (LES) model coupled to a multi-layer canopy model to study ozone deposition (hereafter LES-MLC). Recently, LES simulations of canopy turbulence have been performed under varying atmospheric stability (e.g., Patton et al., 2016), and Clifton and Patton (2021) have extended this approach with ozone uptake. These models advantageously resolve turbulent motions at a larger range of length scales, and have an in-canopy vertical resolution on the order of several meters. Therefore, LES models are an appropriate tool to investigate vertical gradients in turbulent exchange inside and directly above forest canopies, and how this affects canopy-atmosphere exchange of NO_x and ozone. As a future line of research, we propose to apply coupled LES-MLC models to improve mechanistic understanding of the interaction between in-canopy turbulent mixing gradients and ozone removal processes. For example, LES-MLC models can be applied to investigate how vegetated canopies affect chemical ozone flux divergence (Vila-Guerau De Arel-

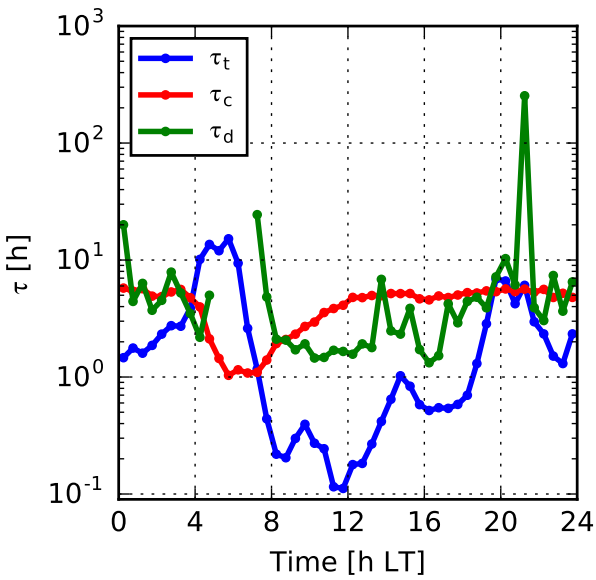

Figure 10. Campaign-averaged diurnal cycles of lifetimes against vertical transport (τ_t), chemical ozone loss by reaction with NO (τ_c) and deposition (τ_d) calculated from observations approximately at mid-canopy. Lifetimes are derived as follows: $\tau_t = \frac{1.1|h_c - z|^2}{K_H}$ (Gerken et al., 2017, with z=13m), $\tau_c = \frac{1}{k[NO]}$ (with $k = 1.9 \times 10^{14}$ s^{-1} and [NO] at 8 m), and $\tau_d = \frac{z}{V_d(O_3)}$ (with z=16m). Note that early-morning τ_d values are omitted as they display erratic behavior due to near-zero ozone flux observations.

lano et al., 1993), and to test how this affects the (dis)similarity between vertical diffusivities for sensible heat and trace gases (Fig. S4). This would require performing LES-MLC simulations that closely mimic site conditions at selected observational sites with detailed observations of in-canopy turbulence and trace gas exchange fluxes, which is an area of ongoing research (Bannister et al., 2022). The proposed developments have large potential to improve the representation of turbulent exchange in multi-layer canopy exchange models (e.g. MLC-CHEM) that can be applied in coupled 3D atmospheric chemistry model experiments used for air quality assessments and chemistry-climate studies.

5 Conclusions

We quantified the impact of forest-atmosphere turbulent exchange and soil NO_x exchange on ozone deposition in a polluted Italian forest. To this end, we applied a multi-layer canopy exchange model (MLC-CHEM) to interpret campaign observations of NO_x and ozone mixing ratios, temperature, and fluxes of sensible heat and ozone. Vertical mixing conditions in the dense Bosco Fontana forest canopy are fully or partially decoupled from the overlying air layers during large parts of the campaign, which poses challenges for simulating ozone uptake in multi-layer models of canopy-atmosphere exchange using traditional vertical exchange parameterizations based on K-theory.

We show how turbulent transport can be a limiting factor for ozone deposition to forest canopies. In land surface parameterizations applied in large-scale atmospheric chemistry and transport models, turbulent transport generally does not limit land surface ozone uptake. However, two parameterizations of canopy-atmosphere exchange cannot reproduce the vertical diffusivity derived from observed vertical temperature and sensible heat flux gradients, since they parameterize in-canopy vertical mixing based on above-canopy

wind speed or friction velocity. Accounting for observed vertical exchange in our simulations decreases the simulated deposition velocity by 0.2-0.4 cm s^{-1} (>100%) in the morning when canopy-atmosphere exchange is weak, and a better agreement with observations (-5%) compared to the two tested parameterizations (+10-19%).

The soil contribution to observed in-canopy NO_x mixing ratios is substantial, particularly in the lower canopy layer (45% on average). This is remarkable, given the high background NO_x mixing ratios observed above the canopy (around 4 ppb during daytime). The canopy-atmosphere exchange flux of NO_x at this site, which is dominated by NO_x deposition, is decreased by up to 80% as a result of a significant soil NO_x emission source. However, a sensitivity study showed that the simulated canopy ozone deposition flux is hardly affected by the reaction between ozone and soil-emitted NO. This is partly because the increasing ozone sink posed by the soil NO-ozone reaction leads reduced dry deposition to the soil and understory vegetation, and partly due to enhanced downward ozone transport as the lower canopy becomes a stronger sink.

Our results highlight how the complex nature of vertical mixing in forests affects canopy-atmosphere exchange of reactive trace gases. Including a more physically accurate representation of canopy-atmosphere exchange in atmospheric chemistry modelling on larger spatial scales will help to better quantify the land surface ozone sink, as well as its impacts on surface ozone mixing ratios and ecosystem carbon uptake. In this context, we suggest to apply turbulence-resolving model experiments coupled to multi-layer canopy models of trace gas exchange to support analysis of field observations. This approach has potential to increase our understanding of the interaction between in-canopy turbulence and ozone sinks, and to improve the representation thereof in land surface parameterizations in larger-scale chemistry transport models.

6 Software and data availability

Observations during the intensive ECLAIRE field campaign at Bosco Fontana can be obtained from the following in-text reference: (Owen, 2012). Data used in the creation of Figure 1 can be obtained from the following in-text references: (Beguería, 2017; Holmes & Ducker, 2018). The MLC-CHEM model version and model output used in this study are stored at the 4TU.ResearchData repository (private link: `https://figshare.com/s/79ac1383e54079145cf8`, a DOI has been reserved and will be shared upon publication).

Acknowledgments

AJV thanks Jordi Vilà-Guerau de Arellano for the discussions that led to the conception of this study. AJV was supported by the Dutch Research Council (grant no. ALW-GO 16/17). MCK received funding from the European Research Council (ERC) under the European Union's Horizon 2020 research and innovation programme (grant agreement no. 742798). The Bosco Fontana measurement campaign was funded by the European Commision Seventh Framework Programme (collaborative projects "ECLAIRE", grant no. 282910).

References

Ainsworth, E. E. a., Yendrek, C. R., Sitch, S., Collins, W. J., & Emberson, L. D. (2012). The effects of tropospheric ozone on net primary productivity and implications for climate change. *Annual review of plant biology*, *63*(March), 637–61. Retrieved from `http://www.ncbi.nlm.nih.gov/pubmed/22404461` doi: 10.1146/annurev-arplant-042110-103829

Ashworth, K., Chung, S. H., Griffin, R. J., Chen, J., Forkel, R., Bryan, A. M., & Steiner, A. L. (2015). FORest Canopy Atmosphere Transfer (FORCAsT) 1.0:

A 1-D model of biosphere-atmosphere chemical exchange. *Geoscientific Model Development*, *8*(11), 3765–3784. doi: 10.5194/gmd-8-3765-2015

Banerjee, T., & Linn, R. (2018). Effect of vertical canopy architecture on transpiration, Thermoregulation and carbon assimilation. *Forests*, *9*(4). doi: 10.3390/f9040198

Bannister, E. J., MacKenzie, A. R., & Cai, X. (2022). Realistic Forests and the Modeling of Forest-Atmosphere Exchange. *Reviews of Geophysics*, *60*(1), 1–47. doi: 10.1029/2021rg000746

Bates, K. H., & Jacob, D. J. (2020). An Expanded Definition of the Odd Oxygen Family for Tropospheric Ozone Budgets: Implications for Ozone Lifetime and Stratospheric Influence. *Geophysical Research Letters*, *47*(4), 1–9. doi: 10.1029/2019GL084486

Beguería, S. (2017). *SPEIbase: Version 2.5.1 [Dataset].* Zenodo. doi: 10.5281/zenodo.834462

Brown, J. S., Shapkalijevski, M. M., Krol, M. C., Karl, T., Ouwersloot, H. G., Moene, A. F., ... Vilà-Guerau de Arellano, J. (2020). Ozone exchange within and above an irrigated Californian orchard. *Tellus, Series B: Chemical and Physical Meteorology*, *72*(1), 1–17. Retrieved from `https://doi.org/10.1080/16000889.2020.1723346` doi: 10.1080/16000889.2020.1723346

Cionco, R. M. (1978). Analysis of canopy index values for various canopy densities. *Boundary-Layer Meteorology*, *15*, 81–93. doi: 10.1007/BF00165507

Clifton, O. E., Fiore, A. M., Massman, W. J., Baublitz, C. B., Coyle, M., Emberson, L., ... Tai, A. P. (2020). Dry Deposition of Ozone over Land: Processes, Measurement, and Modeling. *Reviews of Geophysics*. doi: 10.1029/2019rg000670

Clifton, O. E., Fiore, A. M., Munger, J. W., Malyshev, S., Horowitz, L. W., Shevliakova, E., ... Griffin, K. L. (2017). Interannual variability in ozone removal by a temperate deciduous forest. *Geophysical Research Letters*, *44*, 542–552. Retrieved from `http://doi.wiley.com/10.1002/2016GL070923` doi: 10.1002/2016GL070923

Clifton, O. E., & Patton, E. G. (2021). Does Organization in Turbulence Influence Ozone Removal by Deciduous Forests? *Journal of Geophysical Research: Biogeosciences*, *126*(6), 1–20. doi: 10.1029/2021JG006362

de Vries, W., Schulte-Uebbing, L., Kros, H., Voogd, J. C., & Louwagie, G. (2021). Spatially explicit boundaries for agricultural nitrogen inputs in the European Union to meet air and water quality targets. *Science of the Total Environment*, *786*, 147283. Retrieved from `https://doi.org/10.1016/j.scitotenv.2021.147283` doi: 10.1016/j.scitotenv.2021.147283

Dorsey, J. R., Duyzer, J. H., Gallagher, M. W., Coe, H., Pilegaard, K., Weststrate, J. H., ... Walton, S. (2004). Oxidized nitrogen and ozone interaction with forests. I : Experimental observations and analysis of exchange with Douglas fir. *Quarterly Journal of the Royal Meteorological Society*, *130*(600 PART A), 1941–1955. doi: 10.1256/qj.03.124

Ducker, J. A., Holmes, C. D., Keenan, T. F., Fares, S., Goldstein, A. H., Mammarella, I., ... Schnell, J. (2018). Synthetic ozone deposition and stomatal uptake at flux tower sites. *Biogeosciences*, *15*, 5395–5413. doi: 10.5194/bg-15-5395-2018

Duyzer, J. H., Dorsey, J. R., Gallagher, M. W., Pilegaard, K., & Walton, S. (2004). Oxidized nitrogen and ozone interaction with forests. II : Multi-layer process-oriented modelling results and a sensitivity study for Douglas fir. *Quarterly Journal of the Royal Meteorological Society*, *130*(600 PART A), 1957–1971. doi: 10.1256/qj.03.125

El-Madany, T. S., Niklasch, K., & Klemm, O. (2017). Stomatal and non-stomatal turbulent deposition flux of ozone to a managed peatland. *Atmosphere*, *8*(9), 1–16. doi: 10.3390/atmos8090175

Fares, S., Savi, F., Muller, J., Matteucci, G., & Paoletti, E. (2014). Simulta-

neous measurements of above and below canopy ozone fluxes help partitioning ozone deposition between its various sinks in a Mediterranean Oak Forest. *Agricultural and Forest Meteorology*, *198*, 181–191. Retrieved from `http://dx.doi.org/10.1016/j.agrformet.2014.08.014` doi: 10.1016/j.agrformet.2014.08.014

Fares, S., Weber, R., Park, J. H., Gentner, D., Karlik, J., & Goldstein, A. H. (2012). Ozone deposition to an orange orchard: Partitioning between stomatal and non-stomatal sinks. *Environmental Pollution*, *169*, 258–266. Retrieved from `http://dx.doi.org/10.1016/j.envpol.2012.01.030` doi: 10.1016/j.envpol.2012.01.030

Finco, A., Coyle, M., Nemitz, E., Marzuoli, R., Chiesa, M., Loubet, B., ... Gerosa, G. (2018). Characterization of ozone deposition to a mixed oak-hornbeam forest - Flux measurements at five levels above and inside the canopy and their interactions with nitric oxide. *Atmospheric Chemistry and Physics*, *18*(24), 17945–17961. doi: 10.5194/acp-18-17945-2018

Finnigan, J. J. (2000). Turbulence in plant canopies. *Annual Review of Fluid Mechanics*, *32*, 519–571.

Foken, T., Meixner, F. X., Falge, E., Zetzsch, C., Serafimovich, A., Bargsten, A., ... Zhu, Z. (2012). Coupling processes and exchange of energy and reactive and non-reactive trace gases at a forest site - Results of the EGER experiment. *Atmospheric Chemistry and Physics*, *12*(4), 1923–1950. doi: 10.5194/acp-12-1923-2012

Fowler, D., Pilegaard, K., Sutton, M. A., Ambus, P., Raivonen, M., Duyzer, J., ... Erisman, J. W. (2009). Atmospheric composition change: Ecosystems-Atmosphere interactions. *Atmospheric Environment*, *43*(33), 5193–5267. doi: 10.1016/j.atmosenv.2009.07.068

Galmarini, S., Makar, P., Clifton, O. E., Hogrefe, C., Bash, J., Bellasio, R., ... Wolke, R. (2021). Technical Note - AQMEII4 Activity 1: evaluation of wet and dry deposition schemes as an integral part of regional-scale air quality models. *Atmos. Chem. Phys. Discuss.*. doi: 10.5194/acp-2021-313

Ganzeveld, L. N., Bouwman, L., Stehfest, E., van Vuuren, D., Eickhout, B., & Lelieveld, J. (2010). Impacts of future land cover changes on atmospheric chemistry-climate interactions. *Journal of Geophysical Research*, *115*. doi: 10.1029/2010JD014041

Ganzeveld, L. N., & Lelieveld, J. (1995). Dry deposition parameterization in a chemistry general circulation model and its influence on the distribution of reactive trace gases. *Journal of Geophysical Research*, *100*(D10). doi: 10.1029/95jd02266

Ganzeveld, L. N., Lelieveld, J., Dentener, F. J., Krol, M. C., Bouwman, A. J., & Roelofs, G. J. (2002). Global soil-biogenic NOX emissions and the role of canopy processes. *Journal of Geophysical Research Atmospheres*, *107*(16), 1–17. doi: 10.1029/2001JD001289

Ganzeveld, L. N., Lelieveld, J., Dentener, F. J., Krol, M. C., & Roelofs, G. J. (2002). Atmosphere-biosphere trace gas exchanges simulated with a single-column model. *Journal of Geophysical Research Atmospheres*, *107*(16), 1–21. doi: 10.1029/2001JD000684

Ganzeveld, L. N., Lelieveld, J., & Roelofs, G. J. (1998). A dry deposition parameterization for sulfur oxides in a chemistry and general circulation model. *Journal of Geophysical Research Atmospheres*, *103*(D5), 5679–5694. doi: 10.1029/97JD03077

Gerken, T., Chamecki, M., & Fuentes, J. D. (2017). Air-Parcel Residence Times Within Forest Canopies. *Boundary-Layer Meteorology*, *165*(1), 29–54. doi: 10.1007/s10546-017-0269-7

Gerosa, G., Marzuoli, R., Monteleone, B., Chiesa, M., & Finco, A. (2017). Vertical ozone gradients above forests. Comparison of different calculation options with

direct ozone measurements above a mature forest and consequences for ozone risk assessment. *Forests*, *8*(9). doi: 10.3390/f8090337

Guenther, A. B., Jiang, X., Heald, C. L., Sakulyanontvittaya, T., Duhl, T., Emmons, L. K., & Wang, X. (2012). The model of emissions of gases and aerosols from nature version 2.1 (MEGAN2.1): An extended and updated framework for modeling biogenic emissions. *Geoscientific Model Development*, *5*(6), 1471–1492. doi: 10.5194/gmd-5-1471-2012

Hardacre, C., Wild, O., & Emberson, L. (2015). An evaluation of ozone dry deposition in global scale chemistry climate models. *Atmospheric chemistry and physics*, *15*, 6419–6436. doi: 10.5194/acpd-14-22793-2014

Holmes, C. D., & Ducker, J. A. (2018). *SynFlux: a sythetic dataset of atmospheric deposition and stomatal uptake at flux tower sites (1.1) [Dataset].* Zenodo. doi: https://doi.org/10.5281/zenodo.1402054

Hu, L., Jacob, D. J., Liu, X., Zhang, Y., Zhang, L., Kim, P. S., ... Yantosca, R. M. (2017). Global budget of tropospheric ozone: Evaluating recent model advances with satellite (OMI), aircraft (IAGOS), and ozonesonde observations. *Atmospheric Environment*, *167*, 323–334. doi: 10.1016/j.atmosenv.2017.08.036

Jocher, G., Marshall, J., Nilsson, M. B., Linder, S., De Simon, G., Hörnlund, T., ... Peichl, M. (2018). Impact of Canopy Decoupling and Subcanopy Advection on the Annual Carbon Balance of a Boreal Scots Pine Forest as Derived From Eddy Covariance. *Journal of Geophysical Research: Biogeosciences*, *123*(2), 303–325. doi: 10.1002/2017JG003988

Lin, M., Horowitz, L. W., Xie, Y., Paulot, F., Malyshev, S., Shevliakova, E., ... Pilegaard, K. (2020). Vegetation feedbacks during drought exacerbate ozone air pollution extremes in Europe. *Nature Climate Change*, *10*(May). Retrieved from `http://dx.doi.org/10.1038/s41558-020-0743-y` doi: 10.1038/s41558-020-0743-y

Makar, P. A., Staebler, R. M., Akingunola, A., Zhang, J., McLinden, C., Kharol, S. K., ... Zheng, Q. (2017). The effects of forest canopy shading and turbulence on boundary layer ozone. *Nature Communications*, *8*(May), 1–14. Retrieved from `http://dx.doi.org/10.1038/ncomms15243` doi: 10.1038/ncomms15243

Mölder, M., Grelle, A., Lindroth, A., & Halldin, S. (1999). Flux-profile relationships over a boreal forest - Roughness sublayer corrections. *Agricultural and Forest Meteorology*, *98-99*, 645–658. doi: 10.1016/S0168-1923(99)00131-8

Neirynck, J., Gielen, B., Janssens, I. a., & Ceulemans, R. (2012). Insights into ozone deposition patterns from decade-long ozone flux measurements over a mixed temperate forest. *Journal of Environmental Monitoring*, *14*(6), 1684–95. Retrieved from `http://www.ncbi.nlm.nih.gov/pubmed/22622798` doi: 10.1039/c2em10937a

Owen, S. (2012). *ECLAIRE database [Dataset].* doi: http://eclairedata.ceh.ac.uk/page/login.aspx

Patton, E. G., Sullivan, P. P., Shaw, R. H., Finnigan, J. J., & Weil, J. C. (2016). Atmospheric stability influences on coupled boundary layer and canopy turbulence. *Journal of the Atmospheric Sciences*, *73*(4), 1621–1647. doi: 10.1175/JAS-D-15-0068.1

Pilegaard, K., Skiba, U., Ambus, P., Beier, C., Brüggemann, N., Butterbach-Bahl, K., ... Zechmeister-Boltenstern, S. (2006). Factors controlling regional differences in forest soil emission of nitrogen oxides (NO and N2O). *Biogeosciences*, *3*(4), 651–661. doi: 10.5194/bg-3-651-2006

Rannik, Ü., Altimir, N., Mammarella, I., Bäck, J., Rinne, J., Ruuskanen, T. M., ... Kulmala, M. (2012). Ozone deposition into a boreal forest over a decade of observations: Evaluating deposition partitioning and driving variables. *Atmospheric Chemistry and Physics*, *12*(24), 12165–12182. doi:

10.5194/acp-12-12165-2012

Raupach, M. R. (1989). A practical Lagrangian method for relating scalar concentrations to source distributions in vegetation canopies. *Quarterly Journal of the Royal Meteorological Society*, *115*(487), 609–632. doi: 10.1002/qj.49711548710

Ronda, R., De Bruin, H., & Holtslag, A. (2001). Representation of the canopy conductance in modeling the surface energy budget for low vegetation. *Journal of Applied Meteorology*, *40*, 1431–1444. doi: https://doi.org/10.1175/1520-0450(2001)040⟨1431:ROTCCI⟩2.0.CO;2

Rummel, U., Ammann, C., Kirkman, G. A., Moura, M. A., Foken, T., Andreae, M. O., & Meixner, F. X. (2007). Seasonal variation of ozone deposition to a tropical rain forest in southwest Amazonia. *Atmospheric Chemistry and Physics*, *7*(20), 5415–5435. doi: 10.5194/acp-7-5415-2007

Russell, E. S., Liu, H., Thistle, H., Strom, B., Greer, M., & Lamb, B. (2018). Effects of thinning a forest stand on sub-canopy turbulence. *Agricultural and Forest Meteorology*, *248*(January 2017), 295–305. Retrieved from `https://doi.org/10.1016/j.agrformet.2017.10.019` doi: 10.1016/j.agrformet.2017.10.019

Skiba, U., Medinets, S., Cardenas, L. M., Carnell, E. J., Hutchings, N. J., & Amon, B. (2021). Assessing the contribution of soil NOxemissions to European atmospheric pollution. *Environmental Research Letters*, *16*(2). doi: 10.1088/1748-9326/abd2f2

Steiner, A. L., Pressley, S. N., Botros, A., Jones, E., Chung, S. H., & Edburg, S. L. (2011). Analysis of coherent structures and atmosphere-canopy coupling strength during the CABINEX field campaign. *Atmospheric Chemistry and Physics*, *11*(23), 11921–11936. doi: 10.5194/acp-11-11921-2011

Thomas, C., & Foken, T. (2007). Flux contribution of coherent structures and its implications for the exchange of energy and matter in a tall spruce canopy. *Boundary-Layer Meteorology*, *123*(2), 317–337. doi: 10.1007/s10546-006-9144-7

Van Pul, W., & Jacobs, A. (1994). The conductance of a maize crop and the underlying soil to ozone under various environmental conditions. *Boundary-Layer Meteorology*, *69*, 83–99.

Vermeuel, M. P., Cleary, P. A., Desai, A. R., & Bertram, T. H. (2021). Simultaneous Measurements of O3 and HCOOH Vertical Fluxes Indicate Rapid In-Canopy Terpene Chemistry Enhances O3 Removal Over Mixed Temperate Forests. *Geophysical Research Letters*, *48*(3), 1–15. doi: 10.1029/2020GL090996

Vila-Guerau De Arellano, J., Duynkerke, P. G., & Builtjes, P. J. (1993). The divergence of the turbulent diffusion flux in the surface layer due to chemical reactions: the NO-O3-NO2 system. *Tellus, Series B*, *45 B*(1), 23–33. doi: 10.3402/tellusb.v45i1.15576

Vinken, G. C. M., Boersma, K. F., Maasakkers, J. D., Adon, M., & Martin, R. V. (2014). Worldwide biogenic soil NOx emissions inferred from OMI NO2 observations. *Atmospheric Chemistry and Physics*, *14*, 10363–10381. doi: 10.5194/acp-14-10363-2014

Visser, A. J., Boersma, K. F., Ganzeveld, L. N., & Krol, M. C. (2019). European NOx emissions in WRF-Chem derived from OMI: impacts on summertime surface ozone. *Atmospheric Chemistry and Physics*, *19*(18), 11821–11841. doi: 10.5194/acp-2019-295

Visser, A. J., Ganzeveld, L. N., Goded, I., Krol, M. C., Mammarella, I., Manca, G., & Boersma, K. F. (2021). Ozone deposition impact assessments for forest canopies require accurate ozone flux partitioning on diurnal timescales. *Atmospheric Chemistry and Physics*, *21*(24), 18393–18411. doi: 10.5194/acp-21-18393-2021

Willmott, C. (1982). Some comments on the evaluation of model performance. *Bulletin of the American Meteorological Society*, *63*(11), 1309–1313. doi: 10.1175/

1520-0477(1982)063⟨1309:SCOTEO⟩2.0.CO;2

Wu, Z., Schwede, D. B., Vet, R., Walker, J. T., Shaw, M., Staebler, R., & Zhang, L. (2018). Evaluation and Intercomparison of Five North American Dry Deposition Algorithms at a Mixed Forest Site. *Journal of Advances in Modeling Earth Systems*, *10*(7), 1571–1586. doi: 10.1029/2017MS001231

Yienger, J., & Levy, H. (1995). Empirical model of global soil-biogenic NOx emissions. *Journal of Geophysical Research*, *100*(D6), 447–458. doi: 10.1029/95JD00370

Young, P. J., Naik, V., Fiore, A. M., Gaudel, A., Guo, J., Lin, M. Y., ... Zeng, G. (2018). Tropospheric ozone assessment report: Assessment of global-scale model performance for global and regional ozone distributions, variability, and trends. *Elementa*, *6*. doi: 10.1525/elementa.265

Supporting Information for "The combined impact of canopy stability and soil NOx exchange on ozone removal in a temperate deciduous forest"

Auke J. Visser[1], Laurens N. Ganzeveld[1], Angelo Finco[2], Maarten C. Krol[1,3],

Riccardo Marzuoli[2], K. Folkert Boersma[1,4]

[1]Wageningen University, Meteorology and Air Quality Section, Wageningen, the Netherlands

[2]Università Cattolica del Sacro Cuore, Department of Mathematics and Physics, Brescia, Italy

[3]Utrecht University, Institute for Marine and Atmospheric Research Utrecht, Utrecht, the Netherlands

[4]Royal Netherlands Meteorological Institute, R&D Satellite Observations, De Bilt, the Netherlands

Contents of this file

1. Text S1: Spatio-temporal context of ozone deposition

We analyze a synthetic ozone flux data set (SynFlux; Ducker et al., 2018), where the stomatal ozone flux is derived for flux tower eddy covariance measurements based on a combination of inferred stomatal conductance (by inverting the Penman-Monteith equation for flux tower measurements), a gridded dataset of surface ozone concentrations, and a parameterized non-stomatal ozone flux component. Figure 1a shows SynFlux-derived stomatal and total ozone fluxes for summer 2012 (June-August) near North Italy. To place this in a temporal context, we calculate stomatal and total ozone flux anomalies by subtracting the multi-year June-August flux from the June-August 2012 mean flux per site, depicted in Figure 1b.

The ozone flux anomalies in Figure 1b are overlaid on a Standardized Precipitation-Evaporation Index (SPEI) map for June-August 2012. SPEI is a drought index that is based on the difference between precipitation and potential evaporation (Vicente-Serrano et al., 2010). SPEI can be integrated over different timescales; we here use the 6-month SPEI to analyze water deficits occurring over a 6-month time period to capture effects from the onset of the growing season. A 6-month SPEI time series over 1989-2018 is shown in Figure S1. The negative SPEI values in Figure 1b (range: -1.17 - -0.95) indicate a water deficit in summer 2012, but this falls within the 1-σ range of North-Italian summer SPEI-values in the climatological time period. We therefore conclude that the Bosco Fontana observations in summer 2012 are likely representative for typical summer conditions in this region.

References

Ducker, J. A., Holmes, C. D., Keenan, T. F., Fares, S., Goldstein, A. H., Mammarella, I., ... Schnell, J. (2018). Synthetic ozone deposition and stomatal uptake at flux tower sites. *Biogeosciences*, *15*, 5395–5413. doi: 10.5194/bg-15-5395-2018

Finco, A., Coyle, M., Nemitz, E., Marzuoli, R., Chiesa, M., Loubet, B., ... Gerosa, G. (2018). Characterization of ozone deposition to a mixed oak-hornbeam forest - Flux measurements at five levels above and inside the canopy and their interactions with nitric oxide. *Atmospheric Chemistry and Physics*, *18*(24), 17945–17961. doi: 10.5194/acp-18-17945-2018

Vicente-Serrano, S. M., Beguería, S., & López-Moreno, J. I. (2010). A multiscalar drought index sensitive to global warming: The standardized precipitation evapotranspiration index. *Journal of Climate*, *23*(7), 1696–1718. doi: 10.1175/2009JCLI2909.1

Yienger, J., & Levy, H. (1995). Empirical model of global soil-biogenic NOx emissions. *Journal of Geophysical Research*, *100*(D6), 447–458. doi: 10.1029/95JD00370

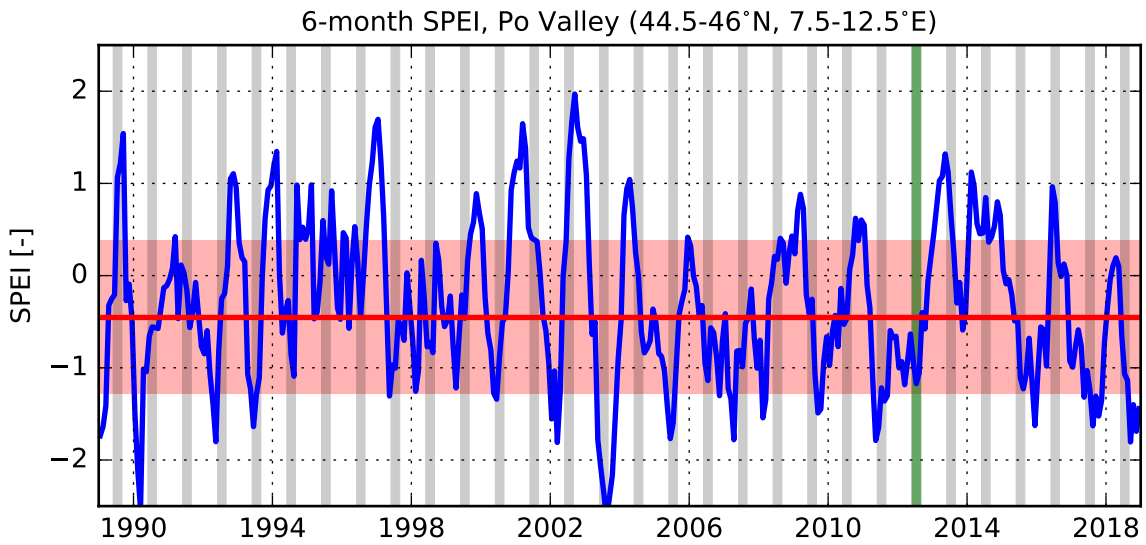

Figure S1. 30-year time series (1989-2018) of the Standardized Precipitation Evaporation Index (SPEI) integrated over the preceding 6 months for the Po Valley in North Italy. Red line and shaded area indicate the June-August mean 6-month SPEI value over the 30-year time series. The green shaded area indicates June-August 2012 when the Bosco Fontana intensive measurement campaign took place.

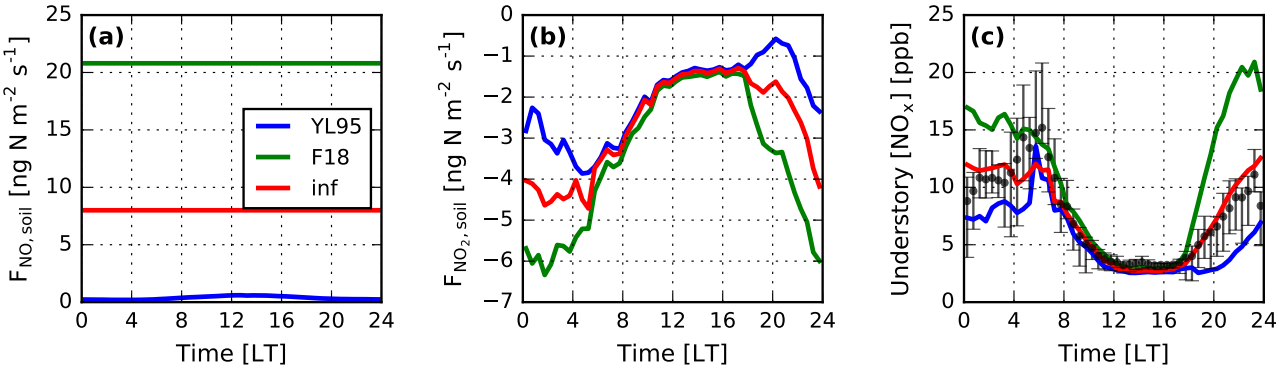

Figure S2. Diurnally averaged soil fluxes of NO (panel a) for different MLC-CHEM runs during July 2012 in Bosco Fontana, based on default MLC-CHEM emissions factors for deciduous forests (blue line; Yienger & Levy, 1995), the emission strength at Bosco Fontana derived from observations above the forest floor (green line; Finco et al., 2018) and the inferred "effective" soil NO flux representative for the soil impact on simulated mixing ratios at 6.5 m. Panels b and c show the resulting impacts in the diurnal averages of the soil NO_2 deposition flux and NO_x mixing ratios in the understory, respectively. Note that the three MLC-CHEM simulations presented in this figure have been performed with MLC-CHEM's reference parameterization of vertical exchange (REF).

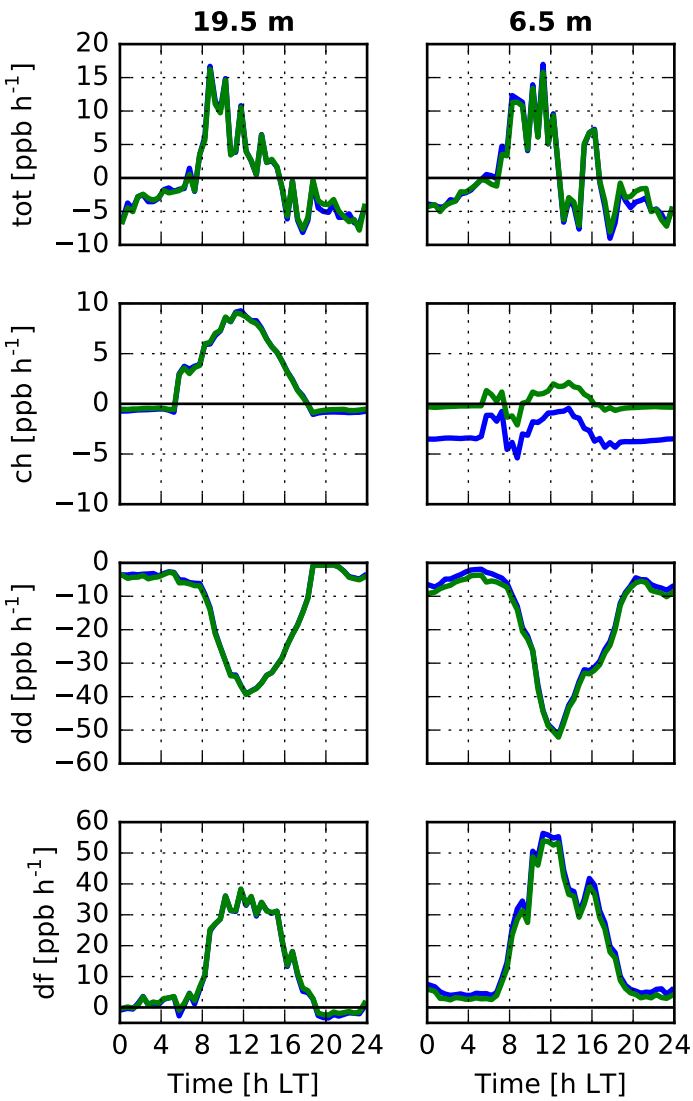

Figure S3. Mean diurnal variation in MLC-CHEM-simulated process tendencies in the upper canopy (19.5 m) and the lower canopy (6.5 m) for the simulations with and without soil NO_x exchange (simulations 4 and 7 in Table 1 in the main text). Tendencies from the following processes are shown: vertical exchange (df), dry deposition (dd), chemistry (ch), and total (tot, i.e., the sum of the previous three tendencies).

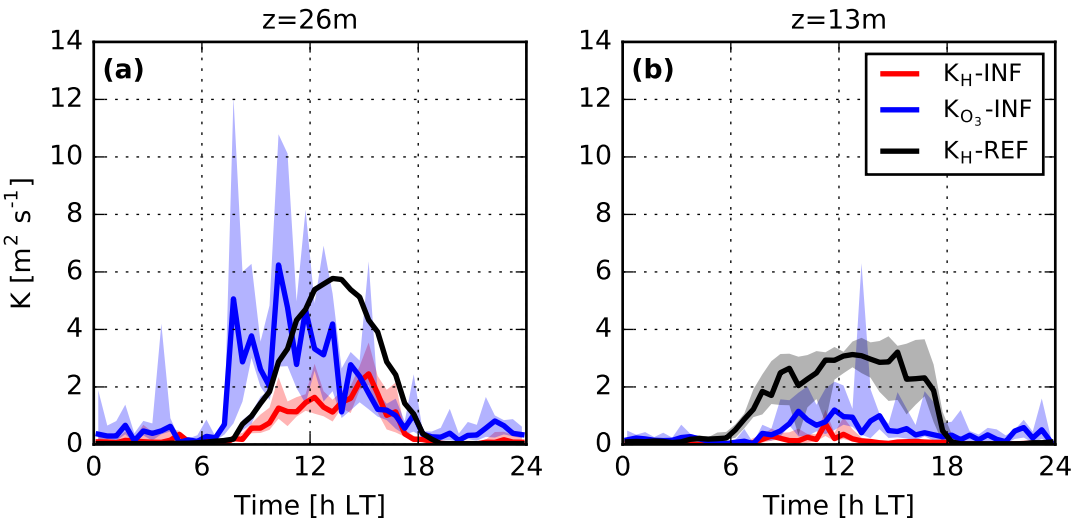

Figure S4. Diurnal variation in vertical diffusivity derived from MLC-CHEM's reference simulation (black line), inferred from sensible heat flux and potential temperature observations (red line), and from vertical profile measurements of the ozone flux and ozone mixing ratios (blue line; obtained by applying Eqn. 2 in the main text for the observed ozone flux and vertical gradient). Solid lines display the campaign median, and shaded areas indicate the inter-quartile range.